http://dx.doi.org/10.5935/0103-5053.20140239

J. Braz. Chem. Soc., Vol. 25, No. 12, 2314-2321, 2014.
Printed in Brazil - ©2014 Sociedade Brasileira de Química
0103 - 5053 $6.00+0.00

Article

Iridium Oxidation States in Catalytic Hydrogenation Intermediates

Janeth Navarro, Marta Martín and Eduardo Sola*

Instituto de Síntesis Química y Catálisis Homogénea (ISQCH), CSIC - Universidad de Zaragoza, E-50009 Zaragoza, Spain

Os conhecidos hidretos de irídio(III) $[IrH_2(NCMe)_3(PiPr_3)]BF_4$, $[IrH(\eta^3\text{-}C_3H_5)(NCMe)_2(PiPr_3)]BF_4$, $[IrH(E\text{-}CH{=}CHPh)(NCMe)_3(PiPr_3)]BF_4$ e $[IrH\{C(Ph){=}CH_2\}(NCMe)_3(PiPr_3)]BF_4$, derivados do precursor catalítico tipo Crabtree $[Ir(cod)(NCMe)(PiPr_3)]BF_4$, foram investigados em reações com substratos tipicamente envolvidos na catálise homogênea de hidrogenação. Novos complexos como as espécies tris-etileno irídio(I) $[Ir(NCMe)(\eta^2\text{-}C_2H_4)_3(PiPr_3)]BF_4$, os produtos de inserção de difenilacetileno $[IrH\{Z\text{-}C(Ph){=}CHPh\}(NCMe)_3(PiPr_3)]BF_4$ e $[Ir(\eta^3\text{-}C_3H_5)\{Z\text{-}C(Ph){=}CHPh\}(NCMe)_2(PiPr_3)]BF_4$, e os derivados de $[Ir(\kappa^2O\text{-acac})(\eta^3\text{-}C_3H_5)\{Z\text{-}C(Ph){=}CHPh\}(PiPr_3)]$ e $[Ir\{\kappa^2C\text{-}C_6H_4\text{-}2\text{-}E\text{-}(CH{=}CPh)\}(NCMe)_3(PiPr_3)]BF_4$, foram caracterizados. O conjunto de observações experimentais sugere que espécies irídio(I), embora acessíveis, são improváveis como intermediários de hidrogenação. Baseados em experimentos de deuteração, uma nova tautomerização do hidreto de alquenil a carbeno foi proposta.

The known iridium(III) hydrides $[IrH_2(NCMe)_3(PiPr_3)]BF_4$, $[IrH(\eta^3\text{-}C_3H_5)(NCMe)_2(PiPr_3)]BF_4$, $[IrH(E\text{-}CH{=}CHPh)(NCMe)_3(PiPr_3)]BF_4$ and $[IrH\{C(Ph){=}CH_2\}(NCMe)_3(PiPr_3)]BF_4$, derived from the Crabtree-type catalyst precursor $[Ir(cod)(NCMe)(PiPr_3)]BF_4$, have been investigated in reactions with substrates typically involved in homogeneous catalytic hydrogenations. New complexes such as the iridium(I) tris-ethylene species $[Ir(NCMe)(\eta^2\text{-}C_2H_4)_3(PiPr_3)]BF_4$, the products of diphenylacetylene insertion $[IrH\{Z\text{-}C(Ph){=}CHPh\}(NCMe)_3(PiPr_3)]BF_4$ and $[Ir(\eta^3\text{-}C_3H_5)\{Z\text{-}C(Ph){=}CHPh\}(NCMe)_2(PiPr_3)]BF_4$, and the derivatives of the latter $[Ir(\kappa^2O\text{-acac})(\eta^3\text{-}C_3H_5)\{Z\text{-}C(Ph){=}CHPh\}(PiPr_3)]$ and $[Ir\{\kappa^2C\text{-}C_6H_4\text{-}2\text{-}E\text{-}(CH{=}CPh)\}(NCMe)_3(PiPr_3)]BF_4$, have been characterized. The set of experimental observations suggests that iridium(I) species, though accessible, are unlikely hydrogenation intermediates. On the basis of deuteration experiments, a new hydride-alkenyl to carbene tautomerization is proposed.

Keywords: homogeneous catalysis, hydrogenation, iridium catalysts, mechanism

Introduction

Iridium homogeneous catalysts have proved suitable for large scale enantioselective hydrogenations of C=N bonds[1] and could soon become industrial also for unfunctionalized olefin substrates.[2] To this end, cationic Crabtree-type catalysts, in particular, are currently under intense investigation to unravel mechanistic details useful for the optimization of ligands and catalysts.[3] Such an investigation is mainly based on theoretical calculations,[4] with just a few experimental contributions.[5] So far, the studies left no doubt that the olefin hydrogenation mechanism involves iridium(III) dihydrides, which are usually observable and often isolable,[5,6] but are less conclusive about whether the catalytic cycle closes via iridium(I) or iridium(V) intermediates.

Fifteen years ago, we reported the cationic iridium(III) dihydride complex $[IrH_2(NCMe)_3(PiPr_3)]BF_4$ (**1**), which was prepared from the Crabtree-type catalyst precursor $[Ir(cod)(NCMe)(PiPr_3)]BF_4$ under conditions typical of homogeneous hydrogenation.[7] This compound turned out to be an adequate precursor for the nuclear magnetic resonance (NMR) observation of organometallic species potentially involved as intermediates in olefin hydrogenation cycles. In fact, we presented possible catalytic cycles for ethylene and propylene hydrogenation totally based on observed intermediates and reaction steps. Since then, our frequent use of this compound as starting material in synthetic work has provided new observations that may contribute to this renewed mechanistic discussion. These observations, presented and discussed in the following pages, suggest that Ir(I) species, though easily accessible, are unlikely hydrogenation intermediates.

*e-mail: sola@unizar.es

Results and Discussion

The dihydride $[IrH_2(NCMe)_3(PiPr_3)]BF_4$ (**1**) was observed to undergo insertion reactions with olefins[7] or alkynes[8] en route to hydrogenation, forming hydride-alkyl or hydride-alkenyl complexes, respectively. The X-ray structure of a representative example of this type of compounds, the product of diphenylacetylene insertion $[IrH\{Z\text{-}C(Ph)=CHPh\}(NCMe)_3(PiPr_3)]BF_4$ (**2**, Scheme 1), is shown in Figure 1. Relevant distances and angles of this structure are listed in Table 1.

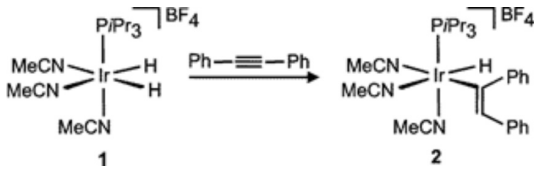

Scheme 1.

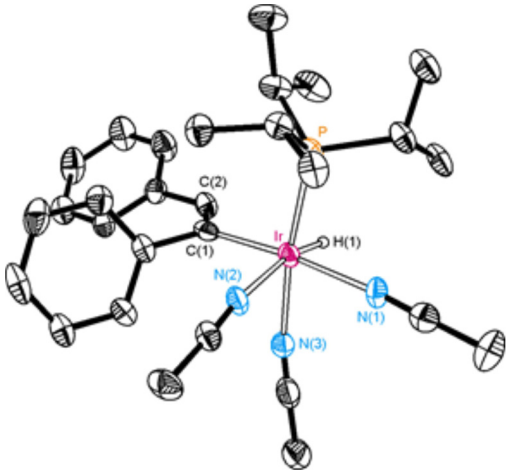

Figure 1. Crystal structure of the cation of complex **2** at the 50% probability level. Hydrogen atoms, except the hydride ligand, are omitted for clarity.

This type of insertion products retain from precursor **1** three easily replaceable acetonitrile ligands, which guarantee further reactivity, and in some cases are stable towards reductive elimination. This is not the case for the labile hydride-alkyl complexes derived from ethylene or propylene insertions, which were reported to readily evolve alkene or alkane via facile H β-eliminations or C-H reductive eliminations, respectively.[7] The hydride-alkenyl complex **2** proved to be more stable than the alkyl derivatives,[9] although it was observed to slowly decompose at room temperature forming *Z*-stilbene, even in the solid state. The reported phenylacetylene analogues of **2**, isomers $[IrH(E\text{-}CH=CHPh)(NCMe)_3(PiPr_3)]BF_4$ (**3-trans**) and $[IrH\{C(Ph)=CH_2\}(NCMe)_3(PiPr_3)]BF_4$ (**3-gem**)[8] (Scheme 2), were found to be rather robust and their study constitutes the first part of this work. In addition, the hydride-η^3-allyl derivative $[IrH(\eta^3\text{-}C_3H_5)(NCMe)_2(PiPr_3)]BF_4$ (**4**),[7] closely related to the hydride-alkyls but less labile due to the additional coordination of the olefin moiety, was also interrogated in the search for possible hydrogenation pathways other than reductive elimination.

As shown in Scheme 2, the treatment of a 1:1 mixture of the hydride-alkenyl isomers **3**[8] with hydrogen (ca. 1 bar) at room temperature readily produced styrene and complex **1**. At low temperature, however, the NMR monitoring of the reaction between these isomers and D_2 revealed deuterium incorporation into the hydride ligand prior to styrene formation. This could be conveniently followed by $^{31}P\{^1H\}$ NMR, given that hydride ligand deuteration produced isotopic shifts of about +0.072 ppm in the phosphorous signal of each isomer **3**. This shift is just slightly smaller than those observed for similar isotopic substitutions in the precursor complex **1** (0.12 ppm).[7] Although such a process scrambles the deuterium label and therefore impede further conclusions about the C–H bond forming step leading to styrene, it clearly indicates that complexes **3** do not need to undergo reductive elimination to cleave the H_2 molecule, in line with the mechanistic alternatives that postulate Ir(V) hydrogenation intermediates.[3]

Scheme 2.

Interestingly, whereas the scrambling of deuterium between D_2 and **3-trans** exclusively involved the hydride ligand, the isomer **3-gem** was observed to further incorporate deuterium into the two geminal positions of the alkenyl ligand. The ^1H and $^{31}P\{^1H\}$ NMR signals of Figure 2, which correspond to a mixture of isotopomers **3-gem** after a few minutes of exposition to D_2 at 253 K, show that the extent of deuterium incorporation into each of the three positions is similar. This could indicate that isomer **3-gem** is in equilibrium with a putative carbene intermediate (Scheme 3), in which methyl rotation statistically distributes the deuterium label into the three positions where it is eventually observed. Given that the process only affects to the gem isomer of **3**, a bulky substituent at the alkenyl

α carbon might be important to achieve this rare hydride-alkenyl to carbene tautomerization. In fact, whereas the protonation of alkenyl complexes is a known synthetic route to carbene derivatives,[10] to the best of our knowledge, an intramolecular version of such reaction has never been reported. Other more conventional explanations for the observed deuteration pattern, in particular those involving styrene formation, can be ruled out because styrene does not react at all with **1** under the conditions of this experiment.

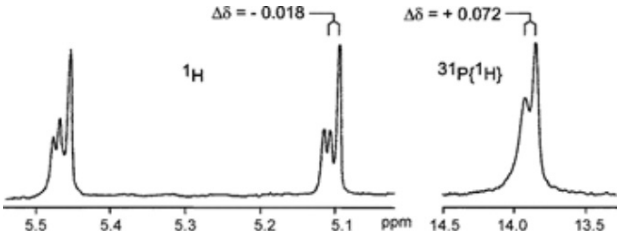

Figure 2. Selected NMR signals of a mixture of isotopomers of **3-gem** in $CDCl_3$ at 253 K: ^1H signals corresponding to the two geminal alkenyl protons (left) and $^{31}P\{^1H\}$ NMR signals (right).

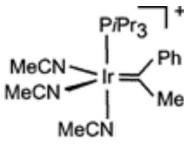

Scheme 3.

In view of the behavior of well-characterized analogues,[11] the proposed intermediate of Scheme 3 should be considered an Ir(I) carbene complex even though it contains a typical Schrock type alkylidene ligand. Unconventional species aside, the experiment of Scheme 2 suggests that other Ir(I) intermediates resulting from reductive eliminations of the hydrogenation products are unlikely in the presence of hydrogen. This conclusion is also consistent with the reported behavior of the hydride-allyl complex **4**, whose reaction with D_2 at room temperature produced propene and the hydride-deuteride isotopomer of **1**.[7] **4** was also tested in reactions with common hydrogen acceptors such as ethylene (Scheme 4).

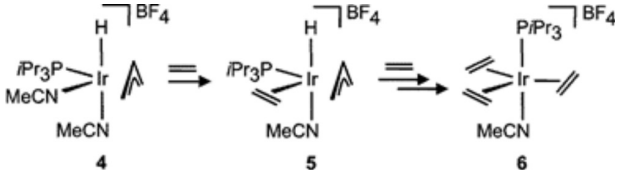

Scheme 4.

The quick exposition to ethylene of a concentrated solution of **4** in chlorinated solvents, followed by a rapid precipitation in diethyl ether, led to the complex $[IrH(\eta^3\text{-}C_3H_5)(NCMe)(\eta^2\text{-}C_2H_4)(P\textit{i}Pr_3)]BF_4$ (**5**, Scheme 4), in which ethylene was incorporated as a ligand instead of one acetonitrile. Note that unlike the reactions with alkynes (see later) and despite the presence of free acetonitrile, the favored product is the hydride-alkene complex instead of an alkyl derivative. Most signals of the NMR spectra of **5** are similar to those of its precursor **4**,[7] including a doublet at δ −29.25 (J_{HP} = 15.0 Hz) in the ^1H spectrum corresponding to a hydride ligand *cis* to phosphorous (and *trans* to acetonitrile) and a doublet at δ 56.61 (J_{CP} = 16.2 Hz) in the $^{13}C\{^1H\}$ spectrum, consistent with an allyllic carbon trans to phosphorous. The new ethylene ligand displays a singlet at δ 44.08 in the $^{13}C\{^1H\}$ NMR spectrum and an AA'BB' spin system at δ 3.23 ($J_{AA'} = J_{BB'}$ = 9.6 Hz, $J_{AB} = J_{A'B'}$ = 8.7 Hz) in the ^1H NMR spectrum, in agreement with the fast rotation of the coordinated ethylene and the lack of symmetry elements in the complex.

More prolonged reactions with ethylene led to solutions whose color changed depending on the amount of dissolved ethylene; being red under vacuum and colorless under ethylene excess. The NMR spectra of these solutions were rather meaningless at any temperature because of the presence of broad signals. Nevertheless, we were able to obtain crystals of what we believe is the major species at low temperature under ethylene excess: the Ir(I) tris-ethylene complex $[Ir(NCMe)(\eta^2\text{-}C_2H_4)_3(P\textit{i}Pr_3)]BF_4$ (**6**). The X-ray structure of this highly symmetric compound is shown in Figure 3, relevant distances and angles are listed in Table 1. The compound displays a regular trigonal bipyramidal structure in which the metal atom is surrounded by six carbons in a planar arrangement, with Ir-C distances in the range 2.20 to 2.24 Å.

The formation of **6** indicates that the excess ethylene is indeed capable of stabilizing the oxidation state Ir(I).

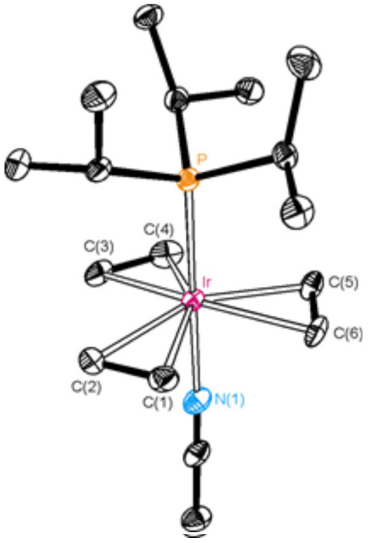

Figure 3. Crystal structure of the cation of complex **6** at the 50% probability level. Hydrogen atoms are omitted for clarity.

The mild reaction conditions leading to this compound also suggest that the replacement of the hard acetonitrile ligands of the Ir(III) precursor by ethylene may facilitate the reductive elimination of propene required to access the Ir(I) intermediates. Yet, the versatility of this type of complexes may enable pathways for propene elimination not necessarily involving Ir(I) intermediates, as suggested by the sequence of reactions in Scheme 5.

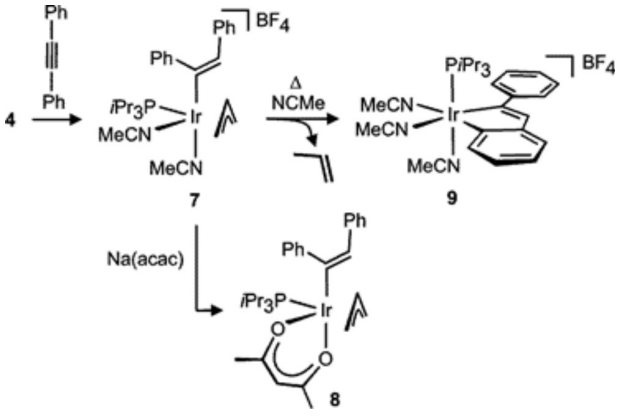

Scheme 5.

Similarly to precursor **1**, complex **4** can undergo insertion of diphenylacetylene into the Ir-H bond to form an alkenyl derivative, [Ir(η^3-C_3H_5){*Z*-C(Ph)=CHPh}$(NCMe)_2$(P*i*Pr_3)]BF_4 (**7**). Although we were not capable of obtaining crystals suitable for a diffraction experiment, the likely structural features of **7** can be inferred in the X-ray structure of its neutral derivative [Ir(κ^2*O*-acac)(η^3-C_3H_5){*Z*-C(Ph)=CHPh}(P*i*Pr_3)] (**8**) (Figure 4 left and Table 1), which was obtained after the replacement of the two labile acetonitrile ligands of **7** by acetylacetonate. The NMR spectra of **8** are consistent with the solid state structure and resemble those of **7**, thus supporting the structural proposal shown in Scheme 5. Both alkenyl-allyl derivatives display characteristic doublets in the $^{13}C\{^1H\}$ NMR spectrum corresponding to alkenyl α carbons *cis* to phosphororus, at δ 124.10 (J_{CP} = 7.2 Hz) for **7** and at δ 129.85 (J_{CP} = 7.5 Hz) for **8**. In addition, as mentioned for **5**, doublets at δ 64.47 (J_{CP} = 20.5 Hz) for **7** and δ 59.22 (J_{CP} = 31.8 Hz) for **8** are diagnostic of the relative *trans* disposition of one of the allyllic carbons and the phosphine.

While derivative **8** is highly stable, its precursor **7** was observed to readily transform at room temperature into the complex [Ir{κ^2*C*-C_6H_4-2-*E*-(CH=CPh)}$(NCMe)_3$(P*i*Pr_3)]BF_4 (**9**), with simultaneous evolution of propene. In view of the structure found for **9** (Figure 4 right and Table 1), the mildness of this transformation is surprising, as it should involve various C-H bond cleavages and formations, not only to enable propene elimination but also to isomerize the former *Z* alkenyl ligand into the *E* form. Such alkenyl ligand isomerizations have been previously observed[12] and seem to play a role in certain catalytic transformations.[13] Typically, they have been attributed to the formation of carbene-like intermediates (zwitterionic or η^2-vinyl),[14] although recent work has disclosed new mechanistic alternatives in iridium complexes.[15] In any case, regardless of the specific mechanism, the transformation of **7** into **9** evidences that these complexes can carry out elaborate transformations of organic molecules without resorting to the oxidation state Ir(I).

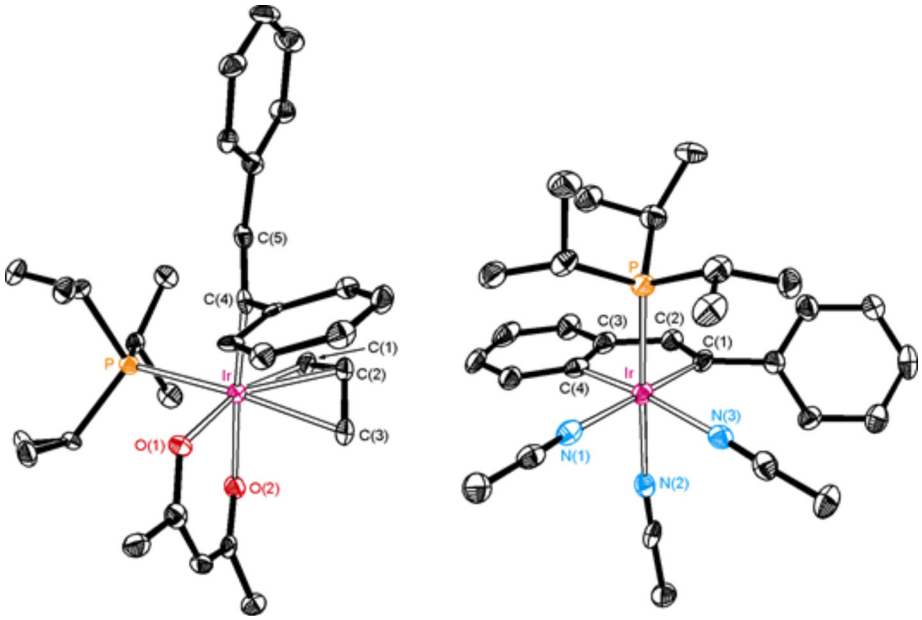

Figure 4. Crystal structures of complex **8** (left) and the cation of complex **9** (right) at the 50% probability level. Hydrogen atoms are omitted for clarity.

Table 1. Selected bond distances (Å) and angles (°) for the X-ray structures

	2	**6**[a]	**8**	**9**
Ir-P	2.2756(14)	2.3209(12)	2.3634(13)	2.3082(15)
Ir-C(1)	2.058(5)	2.239(4)	2.117(5)	2.057(6)
Ir-C(2)	–	2.245(4)	2.141(5)	–
Ir-C(3)	–	2.223(4)	2.208(5)	–
Ir-C(4)	–	2.219(4)	2.048(4)	2.032(6)
Ir-C(5)	–	2.198(4)	–	–
Ir-C(6)	–	2.213(4)	–	–
Ir-N(1)	2.105(4)	2.068(4)	–	2.109(5)
Ir-N(2)	2.147(4)	–	–	2.067(5)
Ir-N(3)	2.084(5)	–	–	2.115(5)
Ir-O(1)	–	–	2.103(3)	–
Ir-O(2)	–	–	2.145(3)	–
C(1)-C(2)	1.346(7)	1.401(6)	1.405(6)	1.340(8)
C(2)-C(3)	–	–	1.408(7)	1.446(8)
C(3)-C(4)	–	1.405(6)	–	1.406(8)
C(5)-C(6)	–	1.411(6)	–	–
P-Ir-C(1)	95.29(14)	95.00(12)	103.59(13)	90.88(15)
P-Ir-C(2)	–	96.81(12)	139.19(13)	–
P-Ir-C(3)	–	95.20(12)	168.32(15)	–
P-Ir-C(4)	–	96.56(13)	95.07(12)	93.93(16)
P-Ir-C(5)	–	94.52(12)	–	–
P-Ir-C(6)	–	96.84(13)	–	–
P-Ir-O(1)	–	–	87.82(8)	–
P-Ir-O(2)	–	–	89.30(9)	–
P-Ir-N(1)	91.50(13)	179.75(11)	–	91.65(13)
P-Ir-N(2)	101.66(13)	–	–	178.13(14)
P-Ir-N(3)	171.79(12)	–	–	95.27(12)
C(1)-C(2)-C(3)	–	–	121.6(5)	116.7(5)

[a]Only one of the two independent molecules in the asymmetric unit is listed.

Conclusions

The set of reactions and new compounds described in this study confirms previous observations indicating that Ir(III) dihydride complexes derived from Crabtree-type catalyst precursors can readily react with hydrogen acceptors (alkenes and alkynes) according to coordination and insertion sequences, although they are less likely to undergo reductive eliminations of the hydrogenated products to form Ir(I) intermediates. As an alternative, the Ir(III) insertion products have proved their ability to cleave H–H and C–H bonds, thus leading to the hydrogenation products without resorting to the oxidation state Ir(I). Nevertheless, the experiments have also allowed observing and proposing Ir(I) intermediates potentially accessible under hydrogenation conditions. One of them, a carbene complex, might result from the rare tautomerization of an Ir(III) hydride-alkenyl derivative.

Experimental

General

All manipulations were carried out with exclusion of air by using standard Schlenk techniques or in an argon-filled drybox (MBraun). Solvents were obtained from a solvent purification system (MBraun). Deuterated solvents were dried with appropriate drying agents and degassed with argon prior to use. C, H and N analyses were carried out in a Perkin-Elmer 2400 CHNS/O analyzer. Mass spectrometry (MS) data were recorded on a VG Autospec double-focusing mass spectrometer operating in the positive mode; ions were produced with the Cs^+ gun at ca. 30 kV, and 3-nitrobenzyl alcohol (NBA) was used as the matrix. Infrared spectra were recorded as Nujol mulls on polyethylene sheets or in KBr using the spectrometers Bruker Equinox 55 or Perkin-Elmer Spectrum One. Conductivities were measured in ca. 3×10^{-4} mol L^{-1} solutions using a Philips PW 9501/01 conductometer. NMR spectra were recorded on Bruker Avance 300 MHz spectrometer. ^{1}H (300.13 MHz) and ^{13}C (75.5 MHz) NMR chemical shifts were measured relative to partially deuterated solvent peaks but are reported in ppm relative to tetramethylsilane (TMS). ^{31}P (121.5 MHz) chemical shifts were measured relative to H_3PO_4 (85%). Coupling constants, *J*, are given in Hertz. In general, NMR spectral assignments were achieved through ^{1}H COSY, ^{1}H NOESY, ^{1}H{^{31}P}, ^{13}C APT, and ^{1}H/^{13}C HSQC experiments. Unless otherwise indicated, the NMR data are given at room temperature.

Synthesis and characterization of the complexes

The complexes **1** and **4**,[7] and the 1:1 mixture of isomers **3-trans** and **3-gem**[8] were prepared following published procedures. All other reagents were commercial and were used as received. The new complexes described below are air-sensitive in solution and solid state.

[IrH(*Z*-C(Ph)=CHPh)$(NCMe)_3$(P*i*Pr_3)]BF_4 (**2**): A solution of **1** (100 mg, 0.18 mmol) in 5 mL of acetone was cooled at 253 K and then treated with diphenylacetylene (48 mg, 0.27 mmol). After 5 min of reaction, the resulting red solution was layered with diethyl ether and stored at 273 K for various days to get pale yellow crystals. The NMR spectra of the crystals revealed the presence of complex **2** and indicated its evolution into *Z*-stilbene and other unidentified compounds. ^{1}H NMR (300.1 MHz, CD_2Cl_2) δ −22.13 (dd, 1H, J_{HP} 21.8 Hz, IrH), 1.17 (dd, 9H, J_{HP} 13.8 Hz, J_{HH} 7.0 Hz, PCHCH_3), 1.25 (dd, 9H, J_{HP} 14.0 Hz, J_{HH} 7.2 Hz, PCHCH_3), 2.41 (m, 3H, PCHCH_3),

2.41 (br, 9H, $NCCH_3$), 6.68 (s, 1H, IrC=C*H*), 6.68 (d, 2H, J_{HH} 7.0 Hz, CH), 6.87 (m, 1H, J_{HH} 7.2 Hz, CH), 6.96 (dd, 2H, J_{HH} 7.2 Hz, 7.0 Hz, CH), 7.05 (m, 3H, CH), 7.13 (m, 2H, CH); $^{31}P\{^1H\}$ NMR (121.5 MHz, CD_2Cl_2) δ 13.10 (s); $^{13}C\{^1H\}$ NMR (75.5 MHz, CD_2Cl_2) δ 3.43, 3.54, 3.67 (all br, NC*C*H_3), 18.57, 19.22 (both d, J_{CP} 2.7 Hz, PCH*C*H_3), 25.00 (d, J_{CP} 26.3 Hz, P*C*HCH$_3$), 118.06, 118.28 (both s, NC*C*H_3), 120.81 (br, NC*C*H_3), 124.67 (d, J_{CP} 2.2 Hz, CH), 125.00, 127.72, 128.82, 129.09, 129.45 (all s, CH) 127.85, 129.35 (both br, CH), 131.44 (d, J_{CP} 7.7 Hz, Ir*C*=CH), 137.57 (d, J_{CP} 7.2 Hz, IrC=*C*H), 142.10, 153.43 (both s, C).

Preparation of [IrH(η^3-C_3H_5)(NCMe)(η^2-C_2H_4)(P*i*Pr$_3$)]BF_4 (**5**): A solution of **4** (100 mg, 0.18 mmol) in CH_2Cl_2 (0.5 mL) was stirred under ethylene atmosphere (ca. 1 bar) during 5 min. The resulting solution was treated with diethyl ether (5 mL) to give a white solid, which was separated by decantation, washed with diethyl ether, and dried *in vacuo*. Yield 89 mg (90%); IR ν/cm^{-1} 2240 (Ir-H); ^1H NMR (300.1 MHz, $CDCl_3$) δ –29.25 (d, 1H, J_{HP} 15.0 Hz, IrH), 1.16, 1.17 (both dd, 9H each, J_{HP} 14.1 Hz, J_{HH} 7.1 Hz, PCHC*H*$_3$), 2.33 (s, 3H, NCC*H*$_3$), 2.45 (d, 1H, J_{HH} 11.1 Hz, η^3-C*H*$_2$CHCH$_2$), 2.58 (m, 3H, PC*H*CH$_3$), 2.88 (dd, 1H, J_{HH} 11.1 Hz, 5.7 Hz, η^3-C*H*$_2$CHCH$_2$), 3.23 (AA'BB' spin system, 4H, δ_A 3.13, δ_B 3.32, J_{AB} $J_{A'B'}$ 8.7 Hz, $J_{AA'}$ $J_{BB'}$ 9.6 Hz, C_2H_4), 3.53, 4.48 (both m, 1H each, η^3-CH$_2$CHC*H*$_2$), 4.84 (m, 1H, η^3-CH$_2$C*H*CH$_2$); $^{31}P\{^1H\}$NMR (212.5 MHz, $CDCl_3$) δ 17.22 (s); $^{13}C\{^1H\}$ NMR (75.5 MHz, $CDCl_3$) δ 2.92 (s, NC*C*H_3), 18.60 (d, J_{CP} 2.7 Hz, PCH*C*H_3), 19.05 (s, PCH*C*H_3), 27.20 (d, J_{CP} 28.6 Hz, P*C*HCH$_3$), 44.08 (s, C_2H_4), 45.06 (d, J_{CP} 2.7 Hz, η^3-*C*H$_2$CHCH$_2$), 56.61 (d, J_{CP} 16.2 Hz, η^3-CH$_2$CH*C*H$_2$), 90.97 (s, η^3-CH$_2$*C*HCH$_2$), 123.20 (s, N*C*CH$_3$); anal. calcd. for $C_{16}H_{34}NBF_4IrP$: C, 34.91; H, 6.23; N, 2.54, found: C, 34.75; H, 6.02; N, 2.62; MS (FAB+, *m/z* (%)) 463 (15) [M$^+$].

[Ir(NCMe)(η^2-C_2H_4)$_3$(P*i*Pr$_3$)]BF_4 (**6**): A solution of **4** (100 mg, 0.18 mmol) in CH_2Cl_2 (5 mL) was stirred under ethylene atmosphere (ca. 1 bar) for 30 min at room temperature. Then, the solution was subjected to vacuum-ethylene cycles until it was concentrated to ca. 0.5 mL. Then it was saturated in ethylene, layered with diethyl ether and stored at 253 K to produce white crystals. ^1H NMR (300.1 MHz, CD_2Cl_2, 273 K) δ 1.14 (dd, 18H, J_{HP} 13.1 Hz, J_{HH} 7.1 Hz, PCHC*H*$_3$), 1.57 (m, 3H, PC*H*CH$_3$), 2.17 (br, 3H, NCCH$_3$), 3.51 (br, η^2-C_2H_4); $^{31}P\{^1H\}$ NMR (121.5 MHz, CD_2Cl_2, 273 K) δ –21.67 (br); $^{13}C\{^1H\}$ NMR (75.5 MHz, CD_2Cl_2, 273 K) δ 3.18 (br, NC*C*H_3), 19.11 (s, PCH*C*H_3), 21.63 (brd, J_{CP} 30.0 Hz, P*C*HCH$_3$), 43.61 (br, C_2H_4).

Preparation of [Ir(η^3-C_3H_5)(*Z*-C(Ph)=CHPh)(NCMe)$_2$(P*i*Pr$_3$)]BF_4 (**7**): A solution of **4** (100 mg, 0.18 mmol) in acetone (1 mL) was treated with PhC≡CPh (48 mg, 0.27 mmol) at 273 K and stirred for 15 min. The resulting red solution was layered with diethyl ether and stored at 263 K. After 3 days, the microcrystalline white solid obtained was separated by decantation, washed with diethyl ether and dried *in vacuo*. Yield 87 mg (65%); ^1H NMR (300.1 MHz, $CDCl_3$, 273 K) δ 1.28 (dd, 9H, J_{HP} 13.8 Hz, J_{HH} 7.2 Hz, PCHC*H*$_3$), 1.42 (dd, 9H, J_{HP} 13.4 Hz, J_{HH} 7.1 Hz, PCHC*H*$_3$), 2.03 (s, 3H, NCCH$_3$), 2.19 (dd, 1H, J_{HH} 10.1 Hz, 3.6 Hz, η^3-C*H*$_2$CHCH$_2$), 2.47 (br, 3H, NCCH$_3$), 2.83 (m, 3H, PC*H*CH$_3$), 3.33 (dd, 1H, J_{HH} 13.1 Hz, 6.6 Hz, η^3-CH$_2$CHC*H*$_2$), 3.52 (d, 1H, J_{HH} 6.6 Hz, η^3-CH$_2$CHC*H*$_2$), 4.67 (dd, 1H, J_{HH} 7.5 Hz, 3.6 Hz, η^3-C*H*$_2$CHCH$_2$), 4.81 (m, 1H, η^3-CH$_2$C*H*CH$_2$), 5.80 (s, 1H, IrC=C*H*), 6.44 (dd, 2H, J_{HH} 8.1 Hz, 1.2 Hz, CH), 6.85 (br, 2H, CH), 6.90 (tt, 1H, J_{HH} 6.9 Hz, 1.2 Hz, CH), 6.94 (dd, 2H, J_{HH} 8.1 Hz, 6.9 Hz, CH), 7.10 (brt, 1H, CH), 7.25 (br, 2H, CH); $^{31}P\{^1H\}$ NMR (121.5 MHz, $CDCl_3$) δ 5.93 (s); $^{13}C\{^1H\}$ NMR (75.5 MHz, $CDCl_3$, 273 K) δ 2.88 (s, NC*C*H_3), 3.36 (br, NC*C*H_3), 19.25, 19.31 (both s, PCH*C*H_3), 25.00 (d, J_{CP} 26.3 Hz, P*C*HCH$_3$), 26.00 (s, η^3-*C*H$_2$CHCH$_2$), 64.47 (d, J_{CP} 20.5 Hz, η^3-CH$_2$CH*C*H$_2$), 107.49 (s, η^3-CH$_2$*C*HCH$_2$), 122.47 (s, N*C*CH$_3$), 122.95 (br, N*C*CH$_3$), 124.10 (d, J_{CP} 7.2 Hz, Ir*C*=CH), 124.93, 125.28, 126.86, 127.69, 127.96 (all s, CH), 133.07 (d, J_{CP} 4.2 Hz, IrC=*C*H), 139.58, 149.06 (both s, C); anal. calcd. for $C_{30}H_{43}N_2BF_4IrP$: C, 48.58; H, 5.84; N, 3.78, found: C, 48.37; H, 5.73; N, 3.91; MS (FAB+, *m/z* (%)) 655 (10) [M$^+$]; Λ_M (acetone) = 85 Ω^{-1} cm^2 mol^{-1} (1:1).

Preparation of [Ir(κ^2*O*-acac)(η^3-C_3H_5){*Z*-C(Ph)=CHPh}(P*i*Pr$_3$)] (**8**): A solution of Na(acac) (34 mg, 0.28 mmol) in MeOH (1 mL) was added at 273 K to a freshly prepared solution of **7** (100 mg, 0.13 mmol) in MeOH (2 mL). The resulting solution was allowed to reach room temperature and stirred for 30 min. The microcrystalline yellow solid obtained was separated by decantation, washed with MeOH and dried *in vacuo*. Yield 79 mg (90 %); IR ν/cm^{-1} 1570, 1590 (C=O); ^1H NMR (300.1 MHz, $CDCl_3$) δ 1.24, 1.26 (both dd, 9H each, J_{HP} 14.1 Hz, J_{HH} 7.2 Hz, PCHC*H*$_3$), 1.55, 1.62 (both s, 3H each, CH$_3$), 2.01 (brd, 1H, J_{HH} 12.2 Hz, η^3-C*H*$_2$CHCH$_2$), 2.07 (dd, 1H, J_{HH} 12.2 Hz, 8.0 Hz, η^3-C*H*$_2$CHCH$_2$), 2.68 (m, 3H, PC*H*CH$_3$), 3.68 (brd, 1H, J_{HH} 6.9 Hz, η^3-CH$_2$CHC*H*$_2$), 3.89 (dd, 1H, J_{HH} 6.9 Hz, 5.1 Hz, η^3-CH$_2$CHC*H*$_2$), 4.51 (m, 1H, η^3-CH$_2$C*H*CH$_2$), 5.15 (s, 1H, CH), 5.65 (s, 1H, IrC=C*H*), 6.52 (dd, 2H, J_{HH} 8.7 Hz, 1.5 Hz, CH), 6.79 (tt, 1H, J_{HH} 8.7 Hz, 1.5 Hz, CH), 6.91 (t, 2H, J_{HH} 8.7 Hz, CH), 6.96 (m, 2H, CH), 7.02 (m, 3H, CH); $^{31}P\{^1H\}$ NMR (121.5 MHz, $CDCl_3$) δ 11.11 (s); $^{13}C\{^1H\}$ NMR (75.5 MHz, $CDCl_3$) δ 18.77, 19.19 (both s, PCH*C*H_3), 23.57 (d, J_{CP} 23.5 Hz, P*C*HCH$_3$), 27.28 (s, CH$_3$), 27.47 (d, J_{CP} 2.8 Hz, η^3-*C*H$_2$CHCH$_2$), 28.08 (s, CH$_3$), 59.22 (d, J_{CP} 31.8 Hz, η^3-CH$_2$CH*C*H$_2$), 101.59 (s,

CH), 103.68 (s, η^3-CH_2*C*HCH_2), 123.55, 123.85, 126.86, 127.34, 127.97, 128.19 (all s, CH), 129.85 (d, J_{CP} 7.5 Hz, Ir*C*=CH), 133.04 (d, J_{CP} 3.1 Hz, IrC=*C*H), 141.30, 148.68 (both s, C), 185.27, 187.80 (both s, CO); anal. calcd. for $C_{31}H_{44}IrO_2P$: C, 55.42; H, 6.60, found: C, 55.28; H, 6.44. The crystals used in the X-ray diffraction experiment were obtained from a concentrated solution of **8** in MeOH stored at 253 K.

Preparation of [Ir{κ^2*C*-C_6H_4-2-*E*-(CH=CPh)}$(NCMe)_3$(P*i*Pr_3)]BF_4 (**9**): A solution of **7** (100 mg, 0.13 mmol) in CH_2Cl_2 (5 mL) was stirred at room temperature until its colour turned dark red (ca. 30 min.). Then, 12 μL of acetonitrile were added and stirred for 15 more min. The resulting solution was concentrated to 0.5 mL, layered with diethyl ether, and stored at 263 K. The microcrystalline white solid obtained was separated by decantation, washed with diethyl ether and dried *in vacuo*. Yield 60 mg (67%); ^{1}H NMR (300.1 MHz, CD_2Cl_2) δ 0.96, 0.97 (both dd, 9H each, J_{HP} 13.5 Hz, J_{HH} 7.2 Hz, PCHC*H*$_3$), 2.30 (m, 3H, PC*H*CH$_3$), 2.35 (d, 3H, J_{HP} 0.8 Hz, NCCH$_3$), 2.45, 2.62 (both br, 3H each, NCCH$_3$), 6.50 (d, 1H, J_{HP} 0.9 Hz, IrC=C*H*), 6.70 (td, 1H, J_{HH} 7.2 Hz, 1.5 Hz, CH), 6.86 (td, 1H, J_{HH} 7.2 Hz, 1.3 Hz, CH), 6.96 (dd, 1H, J_{HH} 7.2 Hz, 1.3 Hz, CH), 7.17 (tt, 1H, J_{HH} 7.8 Hz, 1.7 Hz, CH), 7.29 (t, 2H, J_{HH} 7.8 Hz, CH), 7.39 (dd, 2H, J_{HH} 7.8 Hz, 1.7 Hz, CH), 7.45 (dd, 1H, J_{HH} 7.1 Hz, 1.3 Hz, CH); ^{31}P{^{1}H} NMR (121.5 MHz, CD_2Cl_2) δ –6.79 (s); ^{13}C{^{1}H} NMR (75.5 MHz, CD_2Cl_2) δ 3.48 (s, NC*C*H$_3$), 3.52 (br, NC*C*H$_3$), 18.98 (d, J_{CP} 2.3 Hz, PCH*C*H$_3$), 19.08 (d, J_{CP} 1.4 Hz, PCH*C*H$_3$), 24.26 (d, J_{CP} 31.7 Hz, P*C*HCH$_3$), 117.11 (d, J_{CP} 17.1 Hz, N*C*CH$_3$), 121.17 (br, N*C*CH$_3$), 121.84, 123.16, 123.65, 134.13, 125.42, 126.98, 127.87 (all s, CH), 135.11, 140.94 (both d, J_{CP} 8.3 Hz, Ir*C*), 144.31 (s, IrC=*C*H), 149.78, 158.76 (both s, C); anal. calcd. for $C_{29}H_{40}N_3BF_4IrP$: C, 47.03; H, 5.44; N, 5.67, found: C, 47.13; H, 5.67; N, 5.41; MS (FAB+, *m/z* (%)) 654 (10) [M$^+$].

Structural analysis of complexes **2**, **6**, **8** and **9**

X-ray data were collected at 100.0(2) K on Bruker SMART APEX area detector diffractometer equipped with a normal focus, 2.4 kW, sealed tube source (molybdenum radiation, λ 0.71073 Å) operating at 50 kV and 30 mA. In all cases, single crystals were mounted on a fiber and covered with protective perfluoropolyether. Each frame covered 0.3° in ω. Data were corrected for absorption by using a multi-scan method applied with the SADABS program.[16] The structures were solved by the Patterson method and refined by full-matrix least squares on F^2 using the Bruker SHELXTL program package,[17] including isotropic and subsequently anisotropic displacement parameters for all non-hydrogen non-disordered atoms. Weighted *R* factors (R_w) and goodness of fit (*S*) are based on F^2, and conventional *R* factors are based on *F*. Hydrogen atoms were included in calculated positions and refined riding on the corresponding carbon atoms, or in observed positions and refined freely. For most of the structures the highest electronic residuals were observed in the proximity of the Ir center and make no chemical sense.

Data for **2**: $C_{29}H_{42}IrN_3PBF_4.1.75(CH_2Cl_2)$; M = 887.73; colorless irregular block, 0.44 × 0.44 × 0.20 mm^3; triclinic, $P\bar{1}$; a = 9.3815(18) Å, b = 14.224(3) Å, c = 14.795(3) Å; α = 87.144(3), β = 87.760(3), γ = 84.327(3); Z = 2; V = 1961.0(6) Å^3; D_c = 1.503 g cm^{-3}; μ = 3.726 mm^{-1}, minimum and maximum transmission factors 0.255 and 0.410; $2\theta_{max}$ = 57.72; 24328 reflections collected, 9334 unique [R(int) = 0.0342]; number of data/restrains/parameters 9334/17/410; final GoF 1.029, $R1$ = 0.0425 [7902 reflections $I > 2\sigma(I)$], $wR2$ = 0.1160 for all data; largest peak and hole 2.151 and –1.407 e Å^{-3}. The hydride ligand was observed and refined with a fixed thermal parameter (10.03) and weak positional restrain (1.59(1) Å: the average value found in the Cambridge Structural Database). The disordered BF_4 was refined with two moieties, complementary occupancy factors, restrained geometry, and isotropic thermal parameters. Two dichloromethane molecules were observed disordered in two positions each, both refined with restrained geometry and isotropic thermal parameters. Their occupancy factors were estimated from the thermal parameters and fixed to 0.50, 0.50 and 0.50 0.25, respectively. The highest electronic residuals were observed in the proximity of the solvent molecules.

Data for **6**: $C_{17}H_{36}IrNPBF_4$, M = 564.47; colorless irregular block, 0.22 × 0.20 × 0.10 mm^3; monoclinic, $P2_1/c$; a = 15.082(2) Å, b = 13.423(2) Å, c = 20.756(3) Å; β = 90.020(3); Z = 8; V = 4201.9(11) Å^3; D_c = 1.785 g cm^{-3}; μ = 6.466 mm^{-1}, minimum and maximum transmission factors 0.330 and 0.564; $2\theta_{max}$ = 57.64; 25356 reflections collected, 9987 unique [R(int) = 0.0359]; number of data/restrains/parameters 9987/0/465; final GoF 1.009, $R1$ = 0.0331 [7993 reflections $I > 2\sigma(I)$], $wR2$ = 0.0711 for all data; largest peak and hole 1.554 and –1.200 e Å^{-3}.

Data for **8**: $C_{31}H_{44}IrO_2P$, M = 671.85; colorless irregular block, 0.16 × 0.14 × 0.12 mm^3; monoclinic, $P2_1$; a = 8.2703(14) Å, b = 17.394(3) Å, c = 10.5830(18) Å; β = 110.955(3); Z = 2; V = 1421.7(4) Å^3; D_c = 1.569 g cm^{-3}; μ = 4.777 mm^{-1}, minimum and maximum transmission

factors 0.532 and 0.617; $2\theta_{max}$ = 56.88; 16659 reflections collected, 6597 unique [R(int) = 0.0327]; number of data/restrains/parameters 6597/7/348; final GoF 0.871, $R1$ = 0.0269 [6008 reflections $I > 2\sigma(I)$], $wR2$ = 0.0450 for all data; largest peak and hole 1.978 and –0.926 e Å^{-3}. Flack parameter results in 0.000(5), which indicates that the absolute structure is correct.

Data for **9**: $C_{29}H_{40}IrN_3PBF_4.C_4H_{10}O$, M = 814.76; colorless irregular block, 0.10 × 0.06 × 0.04 mm^3; triclinic, $P\bar{1}$; a = 10.9216(13) Å, b = 12.3148(14) Å, c = 14.7917(17) Å; α = 98.003(2), β = 97.522(2), γ = 114.742(2); Z = 2; V = 1749.2(4) Å^3; D_c = 1.547 g cm^{-3}; μ = 3.913 mm^{-1}, minimum and maximum transmission factors 0.760 and 0.825; $2\theta_{max}$ = 57.80; 15279 reflections collected, 8125 unique [R(int) = 0.0519]; number of data/restrains/parameters 8125/0/411; final GoF 0.976, $R1$ = 0.0477 [6381 reflections $I > 2\sigma(I)$], $wR2$ = 0.0879 for all data; largest peak and hole 1.420 and –0.953 e Å^{-3}. A crystallization molecule of diethyl ether was observed in the unit cell and refined freely.

Supplementary Information

Supplementary data (NMR spectra of the new compounds) are available free of charge at http://jbcs.sbq.org.br as a PDF file.

CCDC 1023054-1023057 contain the supplementary crystallographic data for this paper. These data can be obtained free of charge from The Cambridge Crystallographic Data Centre via www.ccdc.cam.ac.uk/data_request/cif.

Acknowledgements

This research was supported by the Spanish MINECO (Grants CTQ2009-08023 and CTQ2012-31774).

References

1. Blaser, H.-U. In *Iridium Complexes in Organic Synthesis*; Oro, L. A.; Claver, C., eds.; Wiley-VCH: Weinheim, 2009, pp. 1.
2. Bell, S.; Wüstenberg, B.; Kaiser, S.; Menges, F.; Netscher, T.; Pfaltz, A.; *Science* **2006**, *311*, 642; Roseblade, S. J.; Pfaltz, A.; *Acc. Chem. Res.* **2007**, *40*, 1402.
3. Verendel, J. J.; Pàmies, O.; Diéguez, M.; Andersson, P. G.; *Chem. Rev.* **2014**, *114*, 2130.
4. For recent work with leading references, see: Hopmann, K. H.; Frediani, L.; Bayer, A.; *Organometallics* **2014**, *33*, 2790; Sparta, M.; Riplinger, C.; Neese, F.; *J. Chem. Theory Comput.* **2014**, *10*, 1099.
5. Gruber, S.; Pfaltz, A.; *Angew. Chem., Int. Ed.* **2014**, *53*, 1896; Liu, Y.; Gridnev, I. D.; Zhang, W.; *Angew. Chem., Int. Ed.* **2014**, *53*, 1901; Dietiker, R.; Chen, P.; *Angew. Chem., Int. Ed.* **2004**, *43*, 5513.
6. For examples, see: Gruber, S.; Neuburger, M.; Pfaltz, A.; *Organometallics* **2013**, *32*, 4702; Mazuela, J.; Norrby, P.-O.; Andersson, P. G.; Pámies, O.; Diéguez, M.; *J. Am. Chem. Soc.* **2011**, *133*, 13634; Castillo, M. R.; Martín, M.; Fraile, J. M.; Mayoral, J. A.; Sola, E.; *Angew. Chem., Int. Ed.* **2011**, *50*, 3240; Mazet, C.; Smidt, S. P.; Meuwly, M.; Pfaltz, A.; *J. Am. Chem. Soc.* **2004**, *126,* 14176.
7. Sola, E.; Navarro, J.; López, J. A.; Lahoz, F. J.; Oro, L. A.; Werner, H.; *Organometallics* **1999**, *18*, 3534.
8. Navarro, J.; Sägi , M.; Sola, E.; Lahoz, F. J.; Dobrinovitch, I. T.; Katho, A.; Joó, F.; Oro, L. A.; *Adv. Synth. Catal.* **2003**, *345*, 280.
9. Alkyne insertions are commonly very exothermic and therefore expected to be irreversible in the practice. For a rare exception to this behavior, see: Ghosh, R.; Zhang, X.; Achord, P.; Emge, T. J.; Krogh-Jespersen, K.; Goldman, A. S.; *J. Am. Chem. Soc.* **2007**, *129*, 853.
10. For examples, see: Jung, S.; Ilg, K.; Wolf, J.; Werner, H.; *Organometallics* **2001**, *20*, 2121; Alias, F. M.; Poveda, M. L.; Sellin, M.; Carmona, E.; Gutiérrez-Puebla, E.; Monge, A.; *Organometallics* **1998**, *17*, 4124.
11. Ortmann, D. A.; Weberndörfer, B.; Schöneboom, J.; Werner, H.; *Organometallics* **1999**, *18*, 952; Ortmann, D. A.; Weberndörfer, B.; Ilg, K.; Laubender, M.; Werner, H.; *Organometallics* **2002**, *21*, 2369.
12. See for example: Burns, R. M.; Hubbard, J. L.; *J. Am. Chem. Soc.* **1994**, *116*, 9514 and references therein; Werner, H.; Wolf, J.; Schubert, U.; Ackermann, K.; *J. Organomet. Chem.* **1986**, *317*, 327; Werner, H.; Wolf, J.; Schubert, U.; Ackermann, K.; *J. Organomet. Chem.* **1983**, *243*, C63.
13. Imazaki, Y.; Shirakawa, E.; Ueno, R.; Hayashi, T.; *J. Am. Chem. Soc.* **2012**, *134*, 14760; Crabtree, R. H.; *New J. Chem.* **2003**, *27*, 771; Chung, L. W.; Wu, Y.-D.; Trost, B. M.; Ball, Z. T.; *J. Am. Chem. Soc.* **2003**, *125*, 11578.
14. Frohnapfel, D. S.; Templeton, J. L.; *Coord. Chem. Rev.* **2000**, *206-207*, 199.
15. Ikeda, Y.; Takano, K.; Kodama , S.; Ishii, Y.; *Organometallics* **2014**, *33*, 3998.
16. Blessing, R. H.; *Acta Crystallogr.* **1995**, *A51*, 33-38; *SADABS Area-detector absorption correction*, Bruker AXS Inc., Madison, WI, USA, 1996.
17. *SHELXTL Package v. 6.10*, Bruker AXS Inc., Madison, WI, USA, 2000; Sheldrick, G. M.; *SHELXS-86* and *SHELXL-97*; *Program for Crystal Structure Refinement*; University of Göttingen, Germany, 1997..

Submitted on: August 7, 2014
Published online: October 10, 2014